A machine learning approach to screen for preclinical Alzheimer's disease

Sinead Gaubert, Marion Houot, Federico Raimondo, Manon Ansart, Marie-Constance Corsi, Lionel Naccache, Jacobo Diego Sitt, Marie-Odile Habert, Bruno Dubois, Fabrizio de Vico Fallani, et al.

Title: A machine learning approach to screen for preclinical Alzheimer's disease

Authors:

Sinead Gaubert, MD,[1,2,3] Marion Houot, MSc,[2,4,5] Federico Raimondo, PhD,[1,6] Manon Ansart, PhD,[1,7] Marie-Constance Corsi, PhD,[1,7] Lionel Naccache, MD, PhD,[1,8] Jacobo Diego Sitt, PhD,[1,9,10] Marie-Odile Habert, MD,[11,12,13] Bruno Dubois, MD, PhD,[1,2] Fabrizio De Vico Fallani, PhD,[1,7] Stanley Durrleman, PhD,[1,7] Stéphane Epelbaum, MD, PhD,[1,2,7] for the INSIGHT-preAD study group

1. Institut du Cerveau, ICM, Inserm U 1127, CNRS UMR 7225, Sorbonne Université, F-75013, Paris, France
2. AP-HP, Hôpital Pitié-Salpêtrière, Institute of Memory and Alzheimer's Disease (IM2A), Centre of excellence of neurodegenerative disease (CoEN) and National Reference Centre for Rare or Early Dementias, Department of Neurology, F75013, Paris, France
3. Université de Paris, Lariboisière Fernand-Widal Hospital, Cognitive Neurology Center, Paris, France
4. Center for Clinical Investigation (CIC) Neurosciences, Institut du cerveau et de la Moelle épinière (ICM), F75013, Paris, France
5. Sorbonne Université, AP-HP, GRC n° 21, Alzheimer Precision Medicine (APM), Hôpital de la Pitié-Salpêtrière, Boulevard de l'Hôpital, F-75013, Paris, France
6. Coma Science Group, GIGA-Consciousness, University of Liège, Liège, Belgium
7. Inria, Aramis project-team, F-75013, Paris, France
8. AP-HP, Groupe hospitalier Pitié-Salpêtrière, Department of Neurophysiology, Paris, F-75013, France

9. Cognitive Neuroimaging Unit, Institut National de la Santé et de la Recherche Médicale, U992, F-91191 Gif/Yvette, France

10. NeuroSpin Centre, Institute of BioImaging Commissariat à l'Energie Atomique, F-91191 Gif/Yvette, France

11. Laboratoire d'Imagerie Biomédicale, Sorbonne Universités, UPMC Univ Paris 06, Inserm U1146, CNRS UMR 7371, Paris, France

12. AP-HP, Hôpital Pitié-Salpêtrière, Department of Nuclear Medicine, Paris, F-75013, France

13. Centre d'Acquisition et de Traitement des Images, CATI neuroimaging platform, France (www.cati-neuroimaging.com)

Correspondence should be addressed to: Stéphane Epelbaum, MD, PhD

Hôpital Pitié-Salpêtrière, Institute of Memory and Alzheimer's Disease (IM2A), Department of Neurology, 47-83 Boulevard de l'Hôpital, F75013, Paris, France.

E-mail: stephane.epelbaum@aphp.fr

Telephone: +33 1 42 16 75 22

Fax: +33 1 42 16 75 04

Abstract

Combining multimodal biomarkers could help in the early diagnosis of Alzheimer's disease (AD). We included 304 cognitively normal individuals from the INSIGHT-preAD cohort. Amyloid and neurodegeneration were assessed on ^{18}F-florbetapir and ^{18}F-fluorodeoxyglucose PET, respectively. We used a nested cross-validation approach with non-invasive features (electroencephalography [EEG], APOE4 genotype, demographic, neuropsychological and MRI data) to predict: 1/ amyloid status; 2/ neurodegeneration status; 3/ decline to prodromal AD at 5-year follow-up. Importantly, EEG was most strongly predictive of neurodegeneration, even when reducing the number of channels from 224 down to 4, as 4-channel EEG best predicted neurodegeneration (negative predictive value [NPV] = 82%, positive predictive value [PPV] = 38%, 77% specificity, 45% sensitivity). The combination of demographic, neuropsychological data, APOE4 and hippocampal volumetry most strongly predicted amyloid (80% NPV, 41% PPV, 70% specificity, 58% sensitivity) and most strongly predicted decline to prodromal AD at 5 years (97% NPV, 14% PPV, 83% specificity, 50% sensitivity). Thus, machine learning can help to screen patients at high risk of preclinical AD using non-invasive and affordable biomarkers.

Keywords: Preclinical Alzheimer's disease; Machine learning; Multimodal; EEG; Neurodegeneration.

Abbreviations: A- = amyloid negative; A+ = amyloid positive; EEG = electroencephalography; FCSRT = Free and Cued Selective Reminding Test; INSIGHT-preAD = Investigation of Alzheimer's Predictors in Subjective Memory Complainers; LDA = linear discriminant analysis; MMSE = Mini Mental State Examination; MSF = median spectral frequency; N- = neurodegeneration negative; N+ = neurodegeneration positive; NPV = negative predictive value; PPV = positive predictive value; PSD = power spectral density; SCD = subjective cognitive decline; SUVR = standardised uptake value ratio; SVM = support vector machine; wSMI = weighted symbolic mutual information

1. INTRODUCTION

Alzheimer's disease (AD) brain lesions appear several years before cognitive impairment, during preclinical AD (de Leon et al., 2007). Recent AD trials suggest that patients are more likely to benefit from disease-modifying treatments if treated early in the disease course (Dubois et al., 2016; Jack et al., 2018). Thus, there is an urgent need for reliable, non-invasive and low-cost tools to identify individuals at the earliest stages of AD.

Previous studies have shown that electroencephalography (EEG) metrics could be predictive non-invasive biomarkers for AD (Aghajani et al., 2013; Al-Nuaimi et al., 2018; Babiloni et al., 2018, 2016, 2010; Jeong, 2004; Lehmann et al., 2007; Poil et al., 2013; Yang et al., 2019; Yu et al., 2018). However, most studies have focused on EEG biomarkers at a clinical stage of AD, after the onset of cognitive decline, and not at a preclinical stage.

A recent study demonstrated significant EEG changes in cognitively normal individuals with AD topography-specific neurodegeneration (Gaubert et al., 2019). Thus, quantitative EEG seems to be a promising tool to identify preclinical AD subjects, but further studies are needed to assess the individual diagnostic accuracy.

Furthermore, combining multimodal biomarkers could help in the early diagnosis of AD (Frölich et al., 2017; Gupta et al., 2019; Li et al., 2017; Ritter et al., 2015). Previous studies have proposed multimodal models to predict brain amyloidosis in cognitively normal individuals (Ansart et al., 2020; Insel et al., 2016; Mielke et al., 2012; ten Kate et al., 2018). Being able to accurately predict neurodegeneration would also be important, as biomarkers of neuronal injury appear to best predict future cognitive decline, rather than an abnormal amyloid biomarker alone (Dickerson et al., 2013; Mormino et al., 2014; Soldan et al., 2016).

Our objective was to assess the performance of multimodal non-invasive biomarkers to screen individuals at high risk of preclinical AD, using a machine learning approach. In 304 subjective

cognitive decline (SCD) individuals, we aimed to predict: 1/ amyloid status; 2/ neurodegeneration status; 3/ participants declining to prodromal AD at 5-year follow-up, using their baseline data, in an exploratory analysis.

2. MATERIAL AND METHODS

2.1. Participants

Participants were recruited in the French INSIGHT-preAD cohort, which includes baseline data of 318 cognitively normal individuals, between 70 and 85 years old, with subjective memory complaints but unimpaired cognition (Dubois et al., 2018). Demographic, cognitive, biological, imaging including brain structural and functional MRI, ^{18}F-fluorodeoxyglucose (FDG) PET and ^{18}F-florbetapir PET, EEG and other assessments were performed at baseline and regularly during a 5-year follow-up. 304 subjects were included in this machine learning study, because 14 subjects had missing baseline data. The ethics committee of the Pitié-Salpêtrière Hospital approved the study protocol. Written informed consent according to the Declaration of Helsinki was provided by all participants.

2.2. PET acquisition and processing

PET scans were acquired 50 min after injection of 370 MBq (10 mCi) ^{18}F-florbetapir or 30 min after injection of 2 MBq/kg ^{18}F-FDG. Reconstructed images were analysed with a pipeline developed by the Centre d'Acquisition et Traitement des Images (http://cati-neuroimaging.com). A ^{18}F-florbetapir PET standardised uptake value ratio (SUVR) threshold was set at 0.7918 for positive versus negative amyloid deposition (Dubois et al., 2018). Neurodegeneration status was assessed on ^{18}F-FDG PET scans. Cortical metabolic indices were calculated in four bilateral regions of interest that are specifically affected by AD (Jack et al., 2012): posterior cingulate cortex, inferior parietal lobule, precuneus, and inferior temporal gyrus, and the pons was used as the reference region. Individuals were considered neurodegeneration positive if the mean ^{18}F-

FDG PET SUVR in the four AD-signature regions was below 2.27 (Gaubert et al., 2019). All PET scan data used in this study were acquired at baseline.

2.3. MRI acquisition and processing

MRI scans were obtained over a 1 h period on a 3T Magnetom VERIO system (Siemens Medical Solutions, Erlangen, Germany). Scanning sessions were as follows: three-dimensional T1-weighted magnetisation-prepared rapid gradient echo; two-dimensional fluid-attenuated inversion recovery; two-dimensional T2* diffusion tensor imaging acquisition; T2*-weighted gradient-echo echo-planar series; and a pulsed arterial spin labelling scan for measurement of cerebral blood flow at rest. Hippocampal volume was measured on three-dimensional T1 sequences with our in-house SACHA software, normalised to the mean total intracranial volume.

2.4. EEG acquisition and processing

EEG data were acquired with a high-density 256-channel EGI system (Electrical Geodesics Inc., USA) with a sampling rate of 250 Hz and a vertex reference. 60 seconds of eyes-closed resting-state recording were selected for the analysis. We used a pipeline (Engemann, 2015, 2018; King et al., 2013; Sitt et al., 2014) that automates processing of EEG recordings with artifact removal and extraction of metrics (Gaubert et al., 2019). A band-pass filtering (from 0.5 to 45 Hz) and a notch filter at 50 Hz and 100 Hz were applied. Data were cut into 1 second epochs. Channels that exceeded a 100 µv peak-to-peak amplitude in more than 50% of the epochs were rejected. Channels that exceeded a z-score of four across all the channels mean variance were rejected. This step was repeated two times. Epochs that exceeded a 100 µv peak-to-peak amplitude in more than 10% of the channels were rejected. Channels that exceeded a z-score of four across all the channels mean variance (filtered with a high pass of 25 Hz) were rejected. This step was repeated two times. The remaining epochs were digitally transformed to an average reference. Rejected channels were interpolated.

2.5. Calculation and analysis of EEG metrics

We analysed 304 high-density 256-channel EEG recordings from INSIGHT-preAD baseline data. We calculated 10 EEG metrics that have been shown to be highly relevant for the study of preclinical AD in a previous work (Gaubert et al., 2019): power spectral density (PSD) in delta (1-4 Hz), theta (4-8 Hz), alpha (8-12 Hz), beta (12-30 Hz), gamma (30-45 Hz), median spectral frequency (MSF), spectral entropy, algorithmic complexity and weighted symbolic mutual information (wSMI), a metric of functional connectivity, in theta and alpha band (Gaubert et al., 2019; King et al., 2013; Sitt et al., 2014). EEG metrics were averaged across all epochs. We calculated the mean value of each EEG metric across all scalp electrodes. For the 256-channel EEG setup, scalp (non-facial) electrodes were the first 224 electrodes. All markers were computed using NICE (https://github.com/nice-tools/nice), the NICE pipeline web-implementation (demo.doc-eeg.net) and MNE-Python (Gramfort et al., 2014). The collection of scripts used are publicly available at https://github.com/fraimondo/insight-pread.

2.6. Clinical progression to prodromal AD

Clinical progression to prodromal AD during the 5-year follow-up was defined using the IWG-2 criteria (Dubois et al., 2014). An amnestic syndrome of the hippocampal type or another typical clinical presentation (e.g. logopenic aphasia) (Dubois et al., 2014), persistent on two consecutive visits, at least 6 months apart AND positive amyloid-β deposition on the last ^{18}F-florbetapir PET was categorised as prodromal AD. Medical files were reviewed by an independent committee of experts, who validated the participants' status.

2.7. Statistical analysis

Statistical and machine learning analyses were performed using R 3.6.1. (R Foundation for Statistical Computing, Vienna, Austria. https://www.R-project.org/).

2.7.1. Analysis of baseline characteristics

We compared baseline characteristics between groups using Welch's t test for continuous variables and Fisher's exact test for qualitative variables.

2.7.2. Reduction of the number of electrodes

Reducing the number of electrodes is an essential step to use EEG as a diagnostic tool in clinical practice for preclinical AD detection. We evaluated agreement between mean EEG metrics on 224 electrodes, and using a reduced number of electrodes (128, 64, 32, 16, 8, 4 and 2 electrodes). We calculated intraclass correlation coefficients (ICC) with two-way mixed effects, absolute agreement, single measurement (McGraw and Wong, 1996). Channels were selected so that their configuration was close to a realistic EEG configuration respecting the international 10-20 system, or its 10-10 or 10-5 variants (**Supplementary Figure 1**).

2.8. Machine Learning analysis

We built three models, to predict: 1/ amyloid positive (A+) versus amyloid negative (A-) status; 2/ neurodegeneration positive (N+) versus neurodegeneration negative (N-) status; 3/ participants declining to prodromal AD at 5-year follow-up (AD-decliners) versus cognitively stable individuals (non-decliners), using their baseline data.

2.8.1. Input features

We defined seven groups of features: three EEG groups of features, socio-demographic data, APOE4 status, neuropsychological data and hippocampal volume measured on MRI. The complete list of features is reported in **Table 1**. The following eight combinations of groups of features were compared in the analysis: 1) Socio-demographic and neuropsychological data; 2) Socio-demographic, neuropsychological data, ApoE4 status, and hippocampal volume; 3) 4-channel EEG; 4) 16-channel EEG; 5) 224-channel EEG; 6) 4-channel EEG + combination N°2; 7) 16-channel EEG + combination N°2; 8) 224-channel EEG + combination N°2. For each model

(A+/A-, N+/N-, AD decliners/non-decliners), we first implemented a feature preselection step using student t-test for continuous data or chi-squared test for categorical data to select the five and the ten most significantly different features between each group. In the machine learning analysis, each of the eight combinations of groups of features was tested using: 1) the five best pre-selected features; 2) the ten best pre-selected features; 3) all features, which led to $8 \times 3 = 24$ combinations of features tested.

2.8.2 Machine learning pipeline

We compared three classification algorithms: Random Forest (Breiman, 2001) (R package randomForest version 4.6-14), logistic regression, linear support vector machine (SVM) (Müller et al., 2001) (R package e1071 version 1.7-3). We tuned SVM classifier by optimizing gamma and C-constant parameters. For each model we used the oversampling method (Chawla et al., 2002) to handle the imbalanced datasets and rebalance the class distribution to 50_50%. Predictive performance was evaluated using the following nested cross-validation procedure (**Figure 1**): data was repeatedly (50 times) separated into a training and a test set (85%/15%). The training set was used to find the best algorithm/group of features/pre-selected features combination, which was then applied on the test set on subjects independent of the classifier construction to evaluate the performances. We randomly created 100 bootstrap samples from the training set. A 5-fold cross validation was done for each bootstrap sample. We calculated a median training Youden index for each algorithm/group of features/pre-selected features combination, averaged over the 100 bootstrap samples. The combination with the highest median Youden index was selected in the training part and was then applied on the test set.

2.8.3 Performance measures

The best algorithm/group of features/pre-selected features combination was used on the test set to calculate the following performance measures: area under operating characteristic curve (AUC), sensitivity, specificity, positive predictive value (PPV), negative predictive value (NPV) and

balanced accuracy ([sensitivity + specificity]/2). This procedure was repeated 50 times. Fifty classifiers as well as performance measures were therefore obtained and were summarized with number and percentage or median and quantile 0.025 and 0.975. Finally, the classifier that was most often selected on 50 iterations was considered as the best classifier.

3. RESULTS

3.1. Reduction of the number of electrodes

Evaluation of agreement between mean EEG metrics on 224 electrodes and using a reduced number of electrodes showed excellent agreement for 8 of the 10 EEG metrics when reducing the number of electrodes from 224 down to 4 (ICC > 0.9), for the following EEG metrics: PSD delta, theta, alpha, beta, gamma, MSF, spectral entropy and algorithmic complexity. We found near perfect agreement for the same 8 EEG metrics when reducing the number of electrodes from 224 down to 16 (ICC > 0.98). For wSMI alpha, reliability was good for 128-channel EEG (ICC 0.87 [0.70;0.93]) and poor when reducing the number of channels to 64 and below. For wSMI theta, reliability was poor when reducing the number of channels to 128 and below. Based on these results we created three groups of EEG features for the upcoming machine learning analysis: “224-channel EEG”, “16-channel EEG” and “4-channel EEG” (**Table 1**).

3.2. Prediction of amyloid status

3.2.1. Population characteristics according to amyloid status

At baseline, on 304 participants, 85 subjects were A+ and 219 subjects were A- (**Table 2**). The mean age of all participants was 76.1 years (SD 3.5) and 68.1% of the participants had a high educational level. There were no sex or education differences between A- and A+ groups. Participants in A+ group were older versus A- (76.8 SD 3.5 versus 75.8 SD 3.5, p=0.018). The proportion of APOE4 carriers was higher in A+ versus A- group (36.5% versus 12.8%, p<0.0001). The two groups did not differ for cognitive scores except for Mini Mental State

Examination (MMSE) and Frontal Assessment Battery (FAB) where A+ group had lower scores than A- group (p = 0.03). The mean ^{18}F-FDG PET SUVR did not differ between A+ and A- groups. The total hippocampal volume was lower in A+ versus A- subjects (p=0.002).

3.2.2. Prediction of amyloid status on the test set

3.2.2.1. Best classifier

The best classifier for the prediction of amyloid was random forest with the following combination of groups of features: demographic, neuropsychological data, APOE4 genotype and hippocampal volumetry (with 10 features pre-selected), enabling a median AUC of 0.62, a 62% balanced accuracy, a 58% sensitivity, 70% specificity, a 41% PPV and 80% NPV (**Table 3**).

3.2.2.2. Best features

The best features for the prediction of amyloid were the following (according to the frequency of selection of each feature on 50 iterations): APOE4 genotype (60%), MMSE (60%), hippocampal volumetry (58%), age (52%), FAB (50%), FCSRT Delayed Free Recall (38%), education level (36%), FCSRT Immediate Total Recall (34%), FCSRT Immediate Free Recall (34%), FCSRT Delayed Total Recall (34%) and sex (34%). The other features were selected in a proportion lower than 2%.

3.3. Prediction of neurodegeneration status

3.3.1. Population characteristics according to neurodegeneration status

At baseline, on 304 participants, 72 subjects were N+ and 232 subjects were N- (**Table 4**). There were no age or education differences between groups. There were more women in the N- group (68.1%) compared to the N+ group (45.8%, p<0.0001). The proportion of ApoE4 carriers did not differ between the N+ and N- groups. The two groups did not differ for cognitive scores except for the Free and Cued Selective Reminding Test (FCSRT) delayed free recall where the N+ group

had lower scores (p=0.03). The mean amyloid SUVR was higher in the N+ group (p=0.006). The total hippocampal volume was lower in N+ versus N- subjects (p=0.04).

3.3.2. Prediction of neurodegeneration status on the test set

3.3.2.1. Best classifier

The best classifier for the prediction of neurodegeneration was logistic regression with 4-channel EEG (with five features pre-selected), as this classifier was selected in 38% of 50 iterations, enabling a median AUC of 0.62, a 61% balanced accuracy, a 45% sensitivity, 77% specificity, 38% PPV and 82% NPV (**Table 3**). The second-best classifier was logistic regression with 16-channel EEG (with all variables pre-selected), as this classifier was selected in 36% of 50 iterations, enabling a median AUC of 0.68, a 60% balanced accuracy, a 45% sensitivity, 73% specificity, 34% PPV and 82% NPV.

3.3.2.2. Best features

EEG was the most strongly predictive of neurodegeneration (selected in 100% of 50 iterations). The best EEG features for the prediction of neurodegeneration were the following (according to the frequency of selection of each feature on 50 iterations): 16-channel MSF (54%), 16-channel PSD gamma (54%), 4-channel MSF (38%), 4-channel PSD gamma (38%), 16-channel algorithmic complexity (36%), 16-channel PSD alpha (36%), beta (36%), delta (36%) and theta (36%), and 16-channel spectral entropy (36%). The other features were selected in a proportion lower than 8%.

3.4. Decline to prodromal AD at five-year follow-up

3.4.1. Baseline characteristics of AD-decliners

During the five-year follow-up, 14 individuals declined to prodromal AD and 70 were lost to follow-up (**Table 5**). There were no age, sex or education differences between groups. AD-decliners were more often ApoE4 carriers than non-decliners (57.14% versus 17.95%, p=0.0018).

The 14 AD-decliners had lower baseline FCSRT scores compared to non-decliners. There were no differences between groups regarding the other cognitive scores. All participants declining to prodromal AD were A+ by definition and had higher baseline mean amyloid SUVR compared to non-decliners ($p<0.0001$). Baseline mean ^{18}F-FDG PET SUVR was lower in AD-decliners ($p = 0.023$), with more N+ subjects in the AD-decliner group versus the non-decliner group (50% versus 22.22%, $p = 0.0456$). The baseline total hippocampal volume was lower in AD-decliners versus non-decliners ($p = 0.0005$).

3.4.2. Prediction of decline to prodromal AD: an exploratory analysis

Given the small number of AD-decliners (n=14) at five-year follow-up, the results of this exploratory analysis are described in the supplementary results section.

4. DISCUSSION

To our knowledge, this is the first study combining EEG, APOE4, neuropsychological and MRI data to predict brain amyloidosis and AD topography-specific neurodegeneration in cognitively normal individuals. Moreover, in an exploratory analysis, we set up an algorithm for a 5-year prediction of decline to prodromal AD in cognitively normal elderly memory complainers. Remarkably, EEG was the feature most strongly predictive of neurodegeneration. The combination of demographic, neuropsychological data, APOE4 and hippocampal volumetry most strongly predicted brain amyloidosis and decline to prodromal AD at 5 years follow-up. This work demonstrates how machine learning can help to screen patients at high risk of preclinical AD using non-invasive and affordable biomarkers.

Several studies have focused on EEG biomarkers to classify subjects with prodromal AD or AD dementia versus controls (Aghajani et al., 2013; Al-Nuaimi et al., 2018; Babiloni et al., 2018; Poil et al., 2013; Yang et al., 2019; Yu et al., 2018). However, given the importance of a timely diagnosis to treat patients as early as possible and the shift of clinical trials towards preclinical individuals, it is essential to develop biomarkers to identify patients at an earlier stage of the

disease, before onset of cognitive decline. In this study we analysed a large sample of cognitively normal elderly memory complainers, with a defined amyloid and neurodegeneration status, enabling us to assess the potential of EEG as a screening tool for preclinical AD. In addition to EEG, we assessed other non-invasive features using a multimodal analysis. Importantly, we demonstrated that EEG was the best feature for the prediction of AD topography-specific neurodegeneration. Also, reducing the number of channels from a high-density EEG (224 channels) to a low-density EEG (16-channel and 4-channel EEG) did not alter predictive performance. In fact, the best groups of features to predict neurodegeneration were 4-channel EEG with two frontal and two parietal channels (AUC 0.62, 61% balanced accuracy, 82% NPV, 38% PPV) and 16-channel EEG (AUC 0.68, 60% balanced accuracy, 82% NPV, 34% PPV). Therefore, our approach might be successfully implemented with portable equipment featuring only a few electrodes. Furthermore, 16-channel and 4-channel EEG features only included 8 easy-to-obtain EEG metrics (spectral biomarkers and algorithmic complexity) and for which the collection of scripts is publicly available, thus facilitating future implementation in clinical practice. MSF and PSD gamma were the best EEG features to predict neurodegeneration, which is in line with our previous work showing that neurodegeneration in AD-signature regions translates into a widespread increase of MSF and an increase in high-frequency oscillations in fronto-central regions, these changes having been linked to compensatory mechanisms at the preclinical stage of AD (Gaubert et al., 2019).

Previous studies using resting-state EEG showed accuracies ranging from 77.3% to 98.9% to classify between AD dementia and healthy controls (Aghajani et al., 2013; Al-Nuaimi et al., 2018; Poza et al., 2017; Yang et al., 2019; Yu et al., 2018) and accuracies ranging from 68.5% to 85% to classify between MCI and healthy controls (Babiloni et al., 2018; Poil et al., 2013). Even if some studies show high classification accuracies, results should be interpreted with caution due to small datasets, which can lead to overfitting. Classification between AD dementia and controls generally demonstrates better performance than classification between MCI and controls, which

can be explained by greater contrast between groups in the first case, as AD dementia patients are further advanced in the disease course. Regarding our study, we analysed subjects that were at an earlier stage, as all participants were cognitively normal at baseline. Thus, the obtention of a 61% balanced accuracy, an 82% NPV and a 38% PPV to screen for AD-topography specific neurodegeneration in cognitively normal subjects using solely a low-density 4-channel EEG is promising.

The best combination of groups of features to predict amyloid were demographic (age, education level, sex), neuropsychological data (MMSE, FAB, FCSRT), APOE4 genotype and hippocampal volumetry, enabling a 62% balanced accuracy, an 80% NPV and a 41% PPV. The impact of APOE4 genotype is not surprising, considering that it is the major genetic risk factor for AD (Farrer et al., 1997) and it is related to higher brain amyloid deposition (Reiman et al., 2009). Our findings regarding hippocampal volumetry are consistent with previous studies showing that hippocampal volume reduction is related to higher amyloid burden in cognitively normal elderly subjects (Hsu et al., 2015; Mormino et al., 2009). Regarding the role of neuropsychological data to predict brain amyloidosis, cued memory decline on the FCSRT has previously been linked to elevated amyloid burden in cognitively normal adults (Papp et al., 2017). Concerning MMSE and FAB, our results are in line with a previous meta-analysis showing that increased amyloid burden is associated with lower global cognition scores and executive function in cognitively normal subjects (Hedden et al., 2013), but contrasts with another meta-analysis that found no association of amyloid pathology with MMSE in participants with normal cognition (Jansen et al., 2018). Our results suggest that non-invasive and affordable biomarkers could significantly reduce recruitment costs of A+ subjects in clinical trials. Notably, on 50 iterations, EEG was hardly ever selected for the prediction of amyloid (proportion lower than 2%). An explanation could be that we used averaged EEG metrics across all channels, and chose not to compute several regional EEG metrics, in order to limit the number of features, prevent overfitting and excessive computational time. However, as previous work has shown that amyloid burden could have a

regional effect on EEG signals in cognitively normal individuals (Gaubert et al., 2019; Nakamura et al., 2018), future studies could assess the performance of regional EEG features to predict amyloid. Nevertheless, our work suggests that EEG is a much stronger predictor of neurodegeneration than amyloidosis.

A highlight of this work is the 5-year longitudinal follow-up of SCD patients, enabling us to identify biomarkers associated with progression to prodromal AD. On the 248 individuals of the INSIGHT-preAD cohort that were followed up to 5 years, 14 (5.65%) individuals declined to prodromal AD. The number of AD-decliners was lower than expected, compared to progression rates described in different cohorts following cognitively normal individuals (Parnetti et al., 2019). One hypothesis to explain this low progression rate could be that the majority of participants of the INSIGHT-preAD cohort had a high education level (70%), possibly in relation to the recruitment strategy (volunteer subjects preoccupied by their memory complaints, highly motivated to participate in clinical research protocols), with therefore a supposedly high cognitive reserve providing protective effect on cognitive decline (Pettigrew and Soldan, 2019). A recent study has developed a disease progression model of AD according to education level and demonstrated that higher-educated individuals presented slower progression from SCD to amnestic MCI than lower-educated individuals, while this trend disappeared from amnestic MCI to AD dementia, possibly because of insufficient compensation by cognitive reserve when the pathophysiological burden reaches a severe level (Kim et al., 2020). In an exploratory analysis, we showed that the best classifier for the prediction of decline to prodromal AD was logistic regression with the following combination of groups of features: demographical, neuropsychological data, APOE4 genotype and hippocampal volumetry, enabling a 0.70 AUC, 83% specificity, 50% sensitivity, 97% NPV and 14% PPV. The three most efficient features were FCSRT Immediate Free Recall, closely followed by hippocampal volumetry and APOE4. These results are in line with a previous study showing that FCSRT may be particularly effective in identifying cognitively normal individuals on the AD trajectory at greater risk of clinical

progression (Papp et al., 2017). Our findings regarding the role of hippocampal volumetry are of interest as hippocampal volume calculation is now facilitated by software enabling automatic hippocampal volumetry. Our results argue in favour of hippocampal volumetry as part of routine neuroimaging in memory complainers. Given the small number of AD-decliners in this exploratory analysis, these preliminary results should be interpreted with caution and need to be confirmed in future studies. A number of longitudinal studies have developed multimodal biomarker models to predict future decline to AD dementia in individuals at the MCI stage (Caminiti et al., 2018; Cheng et al., 2015; Gupta et al., 2019; Lin et al., 2020; Moradi et al., 2015; Ritter et al., 2015; Young et al., 2013), but the majority of studies investigating biomarker performances in SCD employ a cross-sectional design in which biomarkers are compared between SCD individuals and healthy controls (Brueggen et al., 2019; López-Sanz et al., 2019; Yan et al., 2019; Zhao et al., 2019), and longitudinal research in this field is still limited. A few studies focused on predicting cognitive decline in individuals with normal cognition or SCD (Bauer et al., 2018; Hays et al., 2020; Scheef et al., 2012; Vogel et al., 2018; Young et al., 2014), but most of them predict non-specific decline in cognitive performance over time (or decline to MCI), but do not predict decline to prodromal AD as defined by the IWG-2 criteria (Dubois et al., 2014) in association with positive amyloid-beta deposition, unlike our study where prodromal AD patients are well-phenotyped, based on clinical and amyloid biomarker criteria. One study by Dumurgier et al. (2017) investigated the relationship between AD biomarkers and subsequent change in cognition in a cohort of cognitively intact older adults during 3-year follow-up and showed that baseline CSF total Tau (t-Tau) and phosphorylated Tau 181 (p-Tau181), in vivo amyloid load, and hippocampal volume were all independently associated with future decline in cognition, with modest predictive performance (AUC = 0.7). Other studies have assessed the diagnostic accuracy of CSF biomarkers and/or amyloid PET to predict cognitive decline in cognitively normal individuals (Donohue et al., 2017; Roe et al., 2013; Soldan et al., 2016), but sampling CSF is an invasive technique and amyloid PET is expensive, which limits their

applicability as routine screening tools in cognitively normal adults. Compared to previous studies, our work, even if exploratory, presents some strengths and degree of novelty, for instance regarding the selected non-invasive biomarkers (e.g. EEG), the targeted population and the long follow-up.

A highpoint of this work is the rigorous machine learning methodology. Repeating the training/testing procedure 50 times enabled us to robustly identify the best classifier and to reliably estimate final performance measures, avoiding obtention of good performance only "by chance" on one iteration. Moreover, we resolved the problem of class imbalance by using the oversampling method to rebalance the class distribution to 50_50%. To confirm that our results would generalize well in a different setting, further studies should replicate our method on an independent cohort of SCD subjects.

A major strength is the prediction of neurodegeneration in addition to amyloid status, while most previous studies focus on predicting amyloid only (Ansart et al., 2020; Insel et al., 2016; Mielke et al., 2012; ten Kate et al., 2018), as the majority of AD trials require only positive amyloid status for enrolment. However, knowing the A and N status of an individual is noteworthy (Jack et al., 2018), because A+N+ individuals are at greater risk of progression to prodromal AD than A+N- individuals (Parnetti et al., 2019). Moreover, characterizing the A and N profile of patients could help to guide treatment, with an ATN biomarker-based participant selection in clinical trials, enabling more homogeneous trial populations (Cummings, 2019). In our study, EEG was the feature most strongly predictive of neurodegeneration on ^{18}F-FDG PET, while one could have expected hippocampal volumetry to be a stronger predictor, as brain atrophy is an accepted neurodegeneration biomarker (Jack et al., 2018). One explanation is that EEG measures brain dysfunction, as does ^{18}F-FDG PET, whereas hippocampal volume is a structural marker. A distinction can be made between "functional" and "structural" neurodegeneration, which are

correlated but not interchangeable. Our results suggest that EEG is a good marker of "functional" neurodegeneration.

A limitation is that pathological Tau marker was not available so we could not develop models to predict T status. Given the good NPV of our models to predict neurodegeneration (NPV 82%), amyloid (NPV 80%) and progression to prodromal AD at 5-year follow-up (NPV 97%), an individual classified as negative (normal) on the 3 predictive models would be at low risk of preclinical AD and future cognitive decline. This individual risk assessment would only require a 1-minute low-density EEG, a blood sample to assess APOE4 status and an MRI for hippocampal volumetry. On the opposite, given the modest PPVs, an individual classified as positive would require close cognitive follow-up and confirmatory exams (e.g. PET-scan), as our approach does not have sufficient diagnostic performance to confirm preclinical AD. Thus, our proposed methodology could be used as an interesting starting point for a screening tool to rule out preclinical AD. Other promising low-invasive biomarkers are currently in development, in particular blood markers, as ultrasensitive immunoassays enable assessment of plasma or serum amyloid-β (Aβ-42 and Aβ-40), t-Tau and p-Tau in a single blood sample (Li and Mielke, 2019). The plasma Aβ-42 level or the Aβ-42/Aβ-40 ratio may have clinical utility for screening elevated brain amyloid deposition (Palmqvist et al., 2019) and plasma p-Tau181 levels have been associated more strongly with both amyloid and tau PET, compared to plasma t-Tau (Mielke et al., 2018). However, it is still uncertain whether the current ultrasensitive technologies will be readily available in clinical laboratories for screening for AD pathology. The translation of blood-based AD biomarkers into routine diagnostic biomarkers will involve many steps.

5. CONCLUSION

This work demonstrates how machine learning can help to screen patients at high risk of preclinical AD using non-invasive and affordable biomarkers, thus optimizing recruitment in clinical trials. Most importantly, it highlights EEG as a promising tool to predict

neurodegeneration with portable equipment featuring only a few electrodes, which paves the way for future application in clinical practice. Moderate classification performances reflect the difficulty of diagnosing AD in SCD patients, a few years before the occurrence of prodromal AD, even with multimodal data and using machine learning. Future studies should combine several preclinical cohorts (Epelbaum et al., 2017) according to a recently published methodology (Gagliardi et al., 2020) and use longitudinal multimodal measurements and polygenic risk scores (Leonenko et al., 2019) to improve predictive performance.

Acknowledgements

We sincerely thank all the staff at the Institut du Cerveau (ICM) and institute for memory and Alzheimer's disease (IM2A) who supported the INSIGHT-preAD project as well as the 318 INSIGHT-preAD volunteers.

Study funding

This work was supported by INSERM in collaboration with ICM, Instituts Hospitalo-Universitaires à ICM, and Pfizer and has received support within the "Investissement d'Avenir" (ANR-10-AIHU-06 and ANR-19-P3IA-0001) programs. The study was promoted in collaboration with the "CHU de Bordeaux" (coordination CIC EC7), the promoter of Memento cohort, funded by the Foundation Plan-Alzheimer. The study was further supported by AVID/Lilly. The funding sources had no role in the study design, data collection, data analysis, or data interpretation.

Conflict of interest statement

S. Gaubert, M. Houot, F. Raimondo, M. Ansart, M-C. Corsi, L. Naccache, J.D. Sitt, B. Dubois, F. De Vico Fallani and S. Durrleman report no relevant disclosures. S. Epelbaum has received honoraria as a speaker or consultant for Eli Lilly, Biogen, Astellas Pharma, Roche and GE Healthcare. M-O. Habert has received fees as a consultant from Blue Earth company.

Appendix A. Supplementary data

Supplementary results; Supplementary Figure 1, Supplementary Table 1.

References

Aghajani, H., Zahedi, E., Jalili, M., Keikhosravi, A., Vahdat, B.V., 2013. Diagnosis of Early Alzheimer's Disease Based on EEG Source Localization and a Standardized Realistic Head Model. IEEE J. Biomed. Health Inform. 17, 1039–1045. https://doi.org/10.1109/JBHI.2013.2253326

Al-Nuaimi, A.H.H., Jammeh, E., Sun, L., Ifeachor, E., 2018. Complexity Measures for Quantifying Changes in Electroencephalogram in Alzheimer's Disease. Complexity 2018, 1–12. https://doi.org/10.1155/2018/8915079

Ansart, M., Epelbaum, S., Gagliardi, G., Colliot, O., Dormont, D., Dubois, B., Hampel, H., Durrleman, S., for the Alzheimer's Disease Neuroimaging Initiative* and the INSIGHT-preAD study, 2020. Reduction of recruitment costs in preclinical AD trials: validation of automatic pre-screening algorithm for brain amyloidosis. Stat. Methods Med. Res. 29, 151–164. https://doi.org/10.1177/0962280218823036

Babiloni, C., Lizio, R., Marzano, N., Capotosto, P., Soricelli, A., Triggiani, A.I., Cordone, S., Gesualdo, L., Del Percio, C., 2016. Brain neural synchronization and functional coupling in Alzheimer's disease as revealed by resting state EEG rhythms. Int. J. Psychophysiol. 103, 88–102. https://doi.org/10.1016/j.ijpsycho.2015.02.008

Babiloni, C., Percio, C.D., Lizio, R., Noce, G., Lopez, S., Soricelli, A., Ferri, R., Pascarelli, M.T., Catania, V., Nobili, F., Arnaldi, D., Famà, F., Orzi, F., Buttinelli, C., Giubilei, F., Bonanni, L., Franciotti, R., Onofrj, M., Stirpe, P., Fuhr, P., Gschwandtner, U., Ransmayr, G., Garn, H., Fraioli, L., Pievani, M., D'Antonio, F., Lena, C.D., Güntekin, B., Hanoğlu, L., Başar, E., Yener, G., Emek-Savaş, D.D., Triggiani, A.I., Taylor, J.P., Pandis, M.F.D., Vacca, L., Frisoni, G.B., Stocchi, F., 2018. Functional cortical source connectivity of resting state electroencephalographic alpha rhythms shows similar abnormalities in patients with mild cognitive impairment due to Alzheimer's and Parkinson's diseases. Clin. Neurophysiol. 129, 766–782. https://doi.org/10.1016/j.clinph.2018.01.009

Babiloni, C., Visser, P.J., Frisoni, G., De Deyn, P.P., Bresciani, L., Jelic, V., Nagels, G., Rodriguez, G., Rossini, P.M., Vecchio, F., Colombo, D., Verhey, F., Wahlund, L.-O., Nobili, F., 2010. Cortical sources of resting EEG rhythms in mild cognitive impairment and subjective memory complaint. Neurobiol. Aging 31, 1787–1798. https://doi.org/10.1016/j.neurobiolaging.2008.09.020

Bauer, C.M., Cabral, H.J., Killiany, R.J., 2018. Multimodal Discrimination between Normal Aging, Mild Cognitive Impairment and Alzheimer's Disease and Prediction of Cognitive Decline. Diagnostics 8. https://doi.org/10.3390/diagnostics8010014

Breiman, L., 2001. Random Forests. Mach. Learn. 45, 5–32.

Brueggen, K., Dyrba, M., Cardenas-Blanco, A., Schneider, A., Fliessbach, K., Buerger, K., Janowitz, D., Peters, O., Menne, F., Priller, J., Spruth, E., Wiltfang, J., Vukovich, R., Laske, C., Buchmann, M., Wagner, M., Röske, S., Spottke, A., Rudolph, J., Metzger, C.D., Kilimann, I., Dobisch, L., Düzel, E., Jessen, F., Teipel, S.J., 2019. Structural integrity in subjective cognitive decline, mild cognitive impairment and Alzheimer's disease based on multicenter diffusion tensor imaging. J. Neurol. 266, 2465–2474. https://doi.org/10.1007/s00415-019-09429-3

Caminiti, S.P., Ballarini, T., Sala, A., Cerami, C., Presotto, L., Santangelo, R., Fallanca, F., Vanoli, E.G., Gianolli, L., Iannaccone, S., Magnani, G., Perani, D., BIOMARKAPD Project, 2018. FDG-PET and CSF biomarker accuracy in prediction of conversion to different dementias in a large multicentre MCI cohort. NeuroImage Clin. 18, 167–177. https://doi.org/10.1016/j.nicl.2018.01.019

Chawla, N.V., Bowyer, K.W., Hall, L.O., Kegelmeyer, W.P., 2002. SMOTE: Synthetic Minority Over-sampling Technique. J. Artif. Intell. Res. 16, 321–357. https://doi.org/10.1613/jair.953

Cheng, B., Liu, M., Zhang, D., Munsell, B.C., Shen, D., 2015. Domain Transfer Learning for MCI Conversion Prediction. IEEE Trans. Biomed. Eng. 62, 1805–1817. https://doi.org/10.1109/TBME.2015.2404809

Cummings, J., 2019. The National Institute on Aging—Alzheimer's Association Framework on Alzheimer's disease: Application to clinical trials. Alzheimers Dement. 15, 172–178. https://doi.org/10.1016/j.jalz.2018.05.006

de Leon, M.J., Mosconi, L., Blennow, K., DeSanti, S., Zinkowski, R., Mehta, P.D., Pratico, D., Tsui, W., Saint Louis, L.A., Sobanska, L., Brys, M., Li, Y., Rich, K., Rinne, J., Rusinek, H., 2007. Imaging and CSF studies in the preclinical diagnosis of Alzheimer's disease. Ann. N. Y. Acad. Sci. 1097, 114–145. https://doi.org/10.1196/annals.1379.012

Dickerson, B.C., Wolk, D.A., Alzheimer's Disease Neuroimaging Initiative, 2013. Biomarker-based prediction of progression in MCI: Comparison of AD signature and hippocampal volume with spinal fluid amyloid-β and tau. Front. Aging Neurosci. 5, 55. https://doi.org/10.3389/fnagi.2013.00055

Donohue, M.C., Sperling, R.A., Petersen, R., Sun, C.-K., Weiner, M.W., Aisen, P.S., for the Alzheimer's Disease Neuroimaging Initiative, 2017. Association Between Elevated Brain Amyloid and Subsequent Cognitive Decline Among Cognitively Normal Persons. JAMA 317, 2305. https://doi.org/10.1001/jama.2017.6669

Dubois, B., Epelbaum, S., Nyasse, F., Bakardjian, H., Gagliardi, G., Uspenskaya, O., Houot, M., Lista, S., Cacciamani, F., Potier, M.-C., Bertrand, A., Lamari, F., Benali, H., Mangin, J.-F., Colliot, O., Genthon, R., Habert, M.-O., Hampel, H., Audrain, C., Auffret, A., Baldacci, F., Benakki, I., Bertin, H., Boukadida, L., Cavedo, E., Chiesa, P., Dauphinot, L., Dos Santos, A., Dubois, M., Durrleman, S., Fontaine, G., Genin, A., Glasman, P., Jungalee, N., Kas, A., Kilani, M., La Corte, V., Lehericy, S., Letondor, C., Levy, M., Lowrey, M., Ly, J., Makiese, O., Metzinger, C., Michon, A., Mochel, F., Poisson, C., Ratovohery, S., Revillon, M., Rojkova, K., Roy, P., Santos-Andrade, K., Schindler, R., Seux, L., Simon, V., Sole, M., Tandetnik, C., Teichmann, M., Thiebaut de Shotten, M., Younsi, N., 2018. Cognitive and neuroimaging features and brain β-amyloidosis in individuals at risk of Alzheimer's disease (INSIGHT-preAD): a longitudinal observational study. Lancet Neurol. 17, 335–346. https://doi.org/10.1016/S1474-4422(18)30029-2

Dubois, B., Feldman, H.H., Jacova, C., Hampel, H., Molinuevo, J.L., Blennow, K., DeKosky, S.T., Gauthier, S., Selkoe, D., Bateman, R., Cappa, S., Crutch, S., Engelborghs, S., Frisoni, G.B., Fox, N.C., Galasko, D., Habert, M.-O., Jicha, G.A., Nordberg, A., Pasquier, F., Rabinovici, G., Robert, P., Rowe, C., Salloway, S., Sarazin, M., Epelbaum, S., de Souza, L.C., Vellas, B., Visser, P.J., Schneider, L., Stern, Y., Scheltens, P., Cummings, J.L., 2014. Advancing research diagnostic criteria for Alzheimer's disease: the IWG-2 criteria. Lancet Neurol. 13, 614–629. https://doi.org/10.1016/S1474-4422(14)70090-0

Dubois, B., Hampel, H., Feldman, H.H., Scheltens, P., Aisen, P., Andrieu, S., Bakardjian, H., Benali, H., Bertram, L., Blennow, K., Broich, K., Cavedo, E., Crutch, S., Dartigues, J.-F., Duyckaerts, C., Epelbaum, S., Frisoni, G.B., Gauthier, S., Genthon, R., Gouw, A.A., Habert, M.-O., Holtzman, D.M., Kivipelto, M., Lista, S., Molinuevo, J.-L., O'Bryant, S.E., Rabinovici, G.D., Rowe, C., Salloway, S., Schneider, L.S., Sperling, R., Teichmann, M., Carrillo, M.C., Cummings, J., Jack, C.R., Proceedings of the Meeting of the International Working Group (IWG) and the American Alzheimer's Association on "The Preclinical State of AD"; July 23, 2015; Washington DC, USA, 2016. Preclinical Alzheimer's disease: Definition, natural history, and diagnostic criteria. Alzheimers Dement. J. Alzheimers Assoc. 12, 292–323. https://doi.org/10.1016/j.jalz.2016.02.002

Dumurgier, J., Hanseeuw, B.J., Hatling, F.B., Judge, K.A., Schultz, A.P., Chhatwal, J.P., Blacker, D., Sperling, R.A., Johnson, K.A., Hyman, B.T., Gómez-Isla, T., 2017. Alzheimer's Disease Biomarkers and Future Decline in Cognitive Normal Older Adults. J. Alzheimers Dis. 60, 1451–1459. https://doi.org/10.3233/JAD-170511

Engemann, D.A., Raimondo, F., King, J.-R., Jas, M., Gramfort, A., Dehaene, S., Naccache, L., Sitt, J., 2015. Automated measurement and prediction of consciousness in vegetative and minimally conscious patients. In: ICML workshop on statistics, machine learning and neuroscience 2015. Lille, France; 2015.

Engemann, D.A., Raimondo, F., King, J.-R., Rohaut, B., Louppe, G., Faugeras, F., Annen, J., Cassol, H., Gosseries, O., Fernandez-Slezak, D., Laureys, S., Naccache, L., Dehaene, S., Sitt, J.D., 2018. Robust EEG-based cross-site and cross-protocol classification of states of consciousness. Brain 141 (11), 3179–3192. https://doi.org/10.1093/brain/awy251

Epelbaum, S., Genthon, R., Cavedo, E., Habert, M.O., Lamari, F., Gagliardi, G., Lista, S., Teichmann, M., Bakardjian, H., Hampel, H., Dubois, B., 2017. Preclinical Alzheimer's disease: A systematic review of the cohorts underlying the concept. Alzheimers Dement. J. Alzheimers Assoc. 13, 454–467. https://doi.org/10.1016/j.jalz.2016.12.003

Farrer, L.A., Cupples, L.A., Haines, J.L., Hyman, B., Kukull, W.A., Mayeux, R., Myers, R.H., Pericak-Vance, M.A., Risch, N., van Duijn, C.M., 1997. Effects of age, sex, and ethnicity on the association between apolipoprotein E genotype and Alzheimer disease. A meta-analysis. APOE and Alzheimer Disease Meta Analysis Consortium. JAMA 278, 1349–1356.

Frölich, L., Peters, O., Lewczuk, P., Gruber, O., Teipel, S.J., Gertz, H.J., Jahn, H., Jessen, F., Kurz, A., Luckhaus, C., Hüll, M., Pantel, J., Reischies, F.M., Schröder, J., Wagner, M., Rienhoff, O., Wolf, S., Bauer, C., Schuchhardt, J., Heuser, I., Rüther, E., Henn, F., Maier, W., Wiltfang, J., Kornhuber, J., 2017. Incremental value of biomarker combinations to predict progression of mild cognitive impairment to Alzheimer's dementia. Alzheimers Res. Ther. 9, 84. https://doi.org/10.1186/s13195-017-0301-7

Gagliardi, G.P., Houot, M., Cacciamani, F., Habert, M.-O., Dubois, B., Epelbaum, S., 2020. The Meta-Memory Ratio: A new cohort-independent way to measure cognitive awareness in asymptomatic individuals at risk for Alzheimer's disease. Alzheimers Res Ther 12, 57. https://doi.org/10.1186/s13195-020-00626-1

Gaubert, S., Raimondo, F., Houot, M., Corsi, M.-C., Naccache, L., Diego Sitt, J., Hermann, B., Oudiette, D., Gagliardi, G., Habert, M.-O., Dubois, B., De Vico Fallani, F., Bakardjian, H., Epelbaum, S., 2019. EEG evidence of compensatory mechanisms in preclinical Alzheimer's disease. Brain 142, 2096–2112. https://doi.org/10.1093/brain/awz150

Gramfort, A., Luessi, M., Larson, E., Engemann, D.A., Strohmeier, D., Brodbeck, C., Parkkonen, L., Hämäläinen, M.S., 2014. MNE software for processing MEG and EEG data. NeuroImage 86, 446–460. https://doi.org/10.1016/j.neuroimage.2013.10.027

Gupta, Y., Lama, R.K., Kwon, G.-R., Alzheimer's Disease Neuroimaging Initiative, 2019. Prediction and Classification of Alzheimer's Disease Based on Combined Features From Apolipoprotein-E Genotype, Cerebrospinal Fluid, MR, and FDG-PET Imaging Biomarkers. Front. Comput. Neurosci. 13. https://doi.org/10.3389/fncom.2019.00072

Hays, C.C., Zlatar, Z.Z., Meloy, M.J., Bondi, M.W., Gilbert, P.E., Liu, T., Helm, J.L., Wierenga, C.E., 2020. Interaction of APOE, cerebral blood flow, and cortical thickness in the entorhinal cortex predicts memory decline. Brain Imaging Behav. 14, 369–382. https://doi.org/10.1007/s11682-019-00245-x

Hedden, T., Oh, H., Younger, A.P., Patel, T.A., 2013. Meta-analysis of amyloid-cognition relations in cognitively normal older adults. Neurology 80, 1341. https://doi.org/10.1212/WNL.0b013e31828ab35d

Hsu, P.J., Shou, H., Benzinger, T., Marcus, D., Durbin, T., Morris, J.C., Sheline, Y.I., 2015. Amyloid burden in cognitively normal elderly is associated with preferential hippocampal

subfield volume loss. J. Alzheimers Dis. JAD 45, 27–33. https://doi.org/10.3233/JAD-141743

Insel, P.S., Palmqvist, S., Mackin, R.S., Nosheny, R.L., Hansson, O., Weiner, M.W., Mattsson, N., 2016. Assessing risk for preclinical β-amyloid pathology with APOE, cognitive, and demographic information. Alzheimers Dement. Amst. Neth. 4, 76–84. https://doi.org/10.1016/j.dadm.2016.07.002

Jack, C.R., Bennett, D.A., Blennow, K., Carrillo, M.C., Dunn, B., Haeberlein, S.B., Holtzman, D.M., Jagust, W., Jessen, F., Karlawish, J., Liu, E., Molinuevo, J.L., Montine, T., Phelps, C., Rankin, K.P., Rowe, C.C., Scheltens, P., Siemers, E., Snyder, H.M., Sperling, R., Elliott, C., Masliah, E., Ryan, L., Silverberg, N., 2018. NIA-AA Research Framework: Toward a biological definition of Alzheimer's disease. Alzheimers Dement. 14, 535–562. https://doi.org/10.1016/j.jalz.2018.02.018

Jack, C.R., Knopman, D.S., Weigand, S.D., Wiste, H.J., Vemuri, P., Lowe, V., Kantarci, K., Gunter, J.L., Senjem, M.L., Ivnik, R.J., Roberts, R.O., Rocca, W.A., Boeve, B.F., Petersen, R.C., 2012. An operational approach to National Institute on Aging-Alzheimer's Association criteria for preclinical Alzheimer disease. Ann. Neurol. 71, 765–775. https://doi.org/10.1002/ana.22628

Jansen, W.J., Ossenkoppele, R., Tijms, B.M., Fagan, A.M., Hansson, O., Klunk, W.E., van der Flier, W.M., Villemagne, V.L., Frisoni, G.B., Fleisher, A.S., Lleó, A., Mintun, M.A., Wallin, A., Engelborghs, S., Na, D.L., Chételat, G., Molinuevo, J.L., Landau, S.M., Mattsson, N., Kornhuber, J., Sabri, O., Rowe, C.C., Parnetti, L., Popp, J., Fladby, T., Jagust, W.J., Aalten, P., Lee, D.Y., Vandenberghe, R., Resende de Oliveira, C., Kapaki, E., Froelich, L., Ivanoiu, A., Gabryelewicz, T., Verbeek, M.M., Sanchez-Juan, P., Hildebrandt, H., Camus, V., Zboch, M., Brooks, D.J., Drzezga, A., Rinne, J.O., Newberg, A., de Mendonça, A., Sarazin, M., Rabinovici, G.D., Madsen, K., Kramberger, M.G., Nordberg, A., Mok, V., Mroczko, B., Wolk, D.A., Meyer, P.T., Tsolaki, M., Scheltens, P., Verhey, F.R.J., Visser, P.J., Aarsland, D., Alcolea, D., Alexander, M., Almdahl, I.S., Arnold, S.E., Baldeiras, I., Barthel, H., van Berckel, B.N.M., Blennow, K., van Buchem, M.A., Cavedo, E., Chen, K., Chipi, E., Cohen, A.D., Förster, S., Fortea, J., Frederiksen, K.S., Freund-Levi, Y., Gkatzima, O., Gordon, M.F., Grimmer, T., Hampel, H., Hausner, L., Hellwig, S., Herukka, S.-K., Johannsen, P., Klimkowicz-Mrowiec, A., Köhler, S., Koglin, N., van Laere, K., de Leon, M., Lisetti, V., Maier, W., Marcusson, J., Meulenbroek, O., Møllergård, H.M., Morris, J.C., Nordlund, A., Novak, G.P., Paraskevas, G.P., Perera, G., Peters, O., Ramakers, I.H.G.B., Rami, L., Rodríguez-Rodríguez, E., Roe, C.M., Rot, U., Rüther, E., Santana, I., Schröder, J., Seo, S.W., Soininen, H., Spiru, L., Stomrud, E., Struyfs, H., Teunissen, C.E., Vos, S.J.B., van Waalwijk van Doorn, L.J.C., Waldemar, G., Wallin, Å.K., Wiltfang, J., Zetterberg, H., 2018. Association of Cerebral Amyloid-β Aggregation With Cognitive Functioning in Persons Without Dementia. JAMA Psychiatry 75, 84–95. https://doi.org/10.1001/jamapsychiatry.2017.3391

Jeong, J., 2004. EEG dynamics in patients with Alzheimer's disease. Clin. Neurophysiol. 115, 1490–1505. https://doi.org/10.1016/j.clinph.2004.01.001

Kim, K.W., Woo, S.Y., Kim, S., Jang, H., Kim, Y., Cho, S.H., Kim, S.E., Kim, S.J., Shin, B.-S., Kim, H.J., Na, D.L., Seo, S.W., 2020. Disease progression modeling of Alzheimer's disease according to education level. Sci. Rep. 10. https://doi.org/10.1038/s41598-020-73911-6

King, J.-R., Sitt, J.D., Faugeras, F., Rohaut, B., El Karoui, I., Cohen, L., Naccache, L., Dehaene, S., 2013. Information Sharing in the Brain Indexes Consciousness in Noncommunicative Patients. Curr. Biol. 23, 1914–1919. https://doi.org/10.1016/j.cub.2013.07.075

Lehmann, C., Koenig, T., Jelic, V., Prichep, L., John, R.E., Wahlund, L.-O., Dodge, Y., Dierks, T., 2007. Application and comparison of classification algorithms for recognition of

Alzheimer's disease in electrical brain activity (EEG). J. Neurosci. Methods 161, 342–350. https://doi.org/10.1016/j.jneumeth.2006.10.023

Leonenko, G., Shoai, M., Bellou, E., Sims, R., Williams, J., Hardy, J., Escott-Price, V., the Alzheimer's Disease Neuroimaging Initiative, 2019. Genetic risk for alzheimer disease is distinct from genetic risk for amyloid deposition. Ann. Neurol. 86, 427–435. https://doi.org/10.1002/ana.25530

Li, D., Mielke, M.M., 2019. An Update on Blood-Based Markers of Alzheimer's Disease Using the SiMoA Platform. Neurol. Ther. 8, 73–82. https://doi.org/10.1007/s40120-019-00164-5

Li, Q., Wu, X., Xu, L., Chen, K., Yao, L., Li, R., 2017. Multi-modal discriminative dictionary learning for Alzheimer's disease and mild cognitive impairment. Comput. Methods Programs Biomed. 150, 1–8. https://doi.org/10.1016/j.cmpb.2017.07.003

Lin, W., Gao, Q., Yuan, J., Chen, Z., Feng, C., Chen, W., Du, M., Tong, T., 2020. Predicting Alzheimer's Disease Conversion From Mild Cognitive Impairment Using an Extreme Learning Machine-Based Grading Method With Multimodal Data. Front. Aging Neurosci. 12, 77. https://doi.org/10.3389/fnagi.2020.00077

López-Sanz, D., Bruña, R., Delgado-Losada, M.L., López-Higes, R., Marcos-Dolado, A., Maestú, F., Walter, S., 2019. Electrophysiological brain signatures for the classification of subjective cognitive decline: towards an individual detection in the preclinical stages of dementia. Alzheimers Res. Ther. 11, 49. https://doi.org/10.1186/s13195-019-0502-3

McGraw, K.O., Wong, S.P., 1996. Forming inferences about some intraclass correlation coefficients. Psychol. Methods 1, 30–46. https://doi.org/10.1037/1082-989X.1.1.30

Mielke, M.M., Hagen, C.E., Xu, J., Chai, X., Vemuri, P., Lowe, V.J., Airey, D.C., Knopman, D.S., Roberts, R.O., Machulda, M.M., Jack, C.R., Petersen, R.C., Dage, J.L., 2018. Plasma phospho-tau181 increases with Alzheimer's disease clinical severity and is associated with tau- and amyloid-positron emission tomography. Alzheimers Dement. 14, 989–997. https://doi.org/10.1016/j.jalz.2018.02.013

Mielke, M.M., Wiste, H.J., Weigand, S.D., Knopman, D.S., Lowe, V.J., Roberts, R.O., Geda, Y.E., Swenson-Dravis, D.M., Boeve, B.F., Senjem, M.L., Vemuri, P., Petersen, R.C., Jack, C.R., 2012. Indicators of amyloid burden in a population-based study of cognitively normal elderly. Neurology 79, 1570–1577. https://doi.org/10.1212/WNL.0b013e31826e2696

Moradi, E., Pepe, A., Gaser, C., Huttunen, H., Tohka, J., Alzheimer's Disease Neuroimaging Initiative, 2015. Machine learning framework for early MRI-based Alzheimer's conversion prediction in MCI subjects. NeuroImage 104, 398–412. https://doi.org/10.1016/j.neuroimage.2014.10.002

Mormino, E.C., Betensky, R.A., Hedden, T., Schultz, A.P., Amariglio, R.E., Rentz, D.M., Johnson, K.A., Sperling, R.A., 2014. Synergistic Effect of β-Amyloid and Neurodegeneration on Cognitive Decline in Clinically Normal Individuals. JAMA Neurol. 71, 1379. https://doi.org/10.1001/jamaneurol.2014.2031

Mormino, E.C., Kluth, J.T., Madison, C.M., Rabinovici, G.D., Baker, S.L., Miller, B.L., Koeppe, R.A., Mathis, C.A., Weiner, M.W., Jagust, W.J., Alzheimer's Disease Neuroimaging Initiative, 2009. Episodic memory loss is related to hippocampal-mediated beta-amyloid deposition in elderly subjects. Brain J. Neurol. 132, 1310–1323. https://doi.org/10.1093/brain/awn320

Müller, K.R., Mika, S., Rätsch, G., Tsuda, K., Schölkopf, B., 2001. An introduction to kernel-based learning algorithms. IEEE Trans. Neural Netw. 12, 181–201. https://doi.org/10.1109/72.914517

Nakamura, A., Cuesta, P., Fernández, A., Arahata, Y., Iwata, K., Kuratsubo, I., Bundo, M., Hattori, H., Sakurai, T., Fukuda, K., Washimi, Y., Endo, H., Takeda, A., Diers, K., Bajo, R., Maestú, F., Ito, K., Kato, T., 2018. Electromagnetic signatures of the preclinical and

prodromal stages of Alzheimer's disease. Brain 141, 1470–1485. https://doi.org/10.1093/brain/awy044

Palmqvist, S., Insel, P.S., Zetterberg, H., Blennow, K., Brix, B., Stomrud, E., the Alzheimer's Disease Neuroimaging Initiative, the Swedish BioFINDER study, Mattsson, N., Hansson, O., 2019. Accurate risk estimation of β-amyloid positivity to identify prodromal Alzheimer's disease: Cross-validation study of practical algorithms. Alzheimers Dement. 15, 194–204. https://doi.org/10.1016/j.jalz.2018.08.014

Papp, K.V., Rentz, D.M., Mormino, E.C., Schultz, A.P., Amariglio, R.E., Quiroz, Y., Johnson, K.A., Sperling, R.A., 2017. Cued memory decline in biomarker-defined preclinical Alzheimer disease. Neurology 88, 1431–1438. https://doi.org/10.1212/WNL.0000000000003812

Parnetti, L., Chipi, E., Salvadori, N., D'Andrea, K., Eusebi, P., 2019. Prevalence and risk of progression of preclinical Alzheimer's disease stages: a systematic review and meta-analysis. Alzheimers Res. Ther. 11, 7. https://doi.org/10.1186/s13195-018-0459-7

Pettigrew, C., Soldan, A., 2019. Defining Cognitive Reserve and Implications for Cognitive Aging. Curr. Neurol. Neurosci. Rep. 19, 1. https://doi.org/10.1007/s11910-019-0917-z

Poil, S.-S., de Haan, W., van der Flier, W.M., Mansvelder, H.D., Scheltens, P., Linkenkaer-Hansen, K., 2013. Integrative EEG biomarkers predict progression to Alzheimer's disease at the MCI stage. Front. Aging Neurosci. 5. https://doi.org/10.3389/fnagi.2013.00058

Poza, J., Gómez, C., García, M., Tola-Arribas, M.A., Carreres, A., Cano, M., Hornero, R., 2017. Spatio-Temporal Fluctuations of Neural Dynamics in Mild Cognitive Impairment and Alzheimer's Disease. Curr. Alzheimer Res. 14. https://doi.org/10.2174/1567205014666170309115656

Reiman, E.M., Chen, K., Liu, X., Bandy, D., Yu, M., Lee, W., Ayutyanont, N., Keppler, J., Reeder, S.A., Langbaum, J.B.S., Alexander, G.E., Klunk, W.E., Mathis, C.A., Price, J.C., Aizenstein, H.J., DeKosky, S.T., Caselli, R.J., 2009. Fibrillar amyloid- burden in cognitively normal people at 3 levels of genetic risk for Alzheimer's disease. Proc. Natl. Acad. Sci. 106, 6820–6825. https://doi.org/10.1073/pnas.0900345106

Ritter, K., Schumacher, J., Weygandt, M., Buchert, R., Allefeld, C., Haynes, J.-D., 2015. Multimodal prediction of conversion to Alzheimer's disease based on incomplete biomarkers. Alzheimers Dement. Amst. Neth. 1, 206–215. https://doi.org/10.1016/j.dadm.2015.01.006

Roe, C.M., Fagan, A.M., Grant, E.A., Hassenstab, J., Moulder, K.L., Maue Dreyfus, D., Sutphen, C.L., Benzinger, T.L.S., Mintun, M.A., Holtzman, D.M., Morris, J.C., 2013. Amyloid imaging and CSF biomarkers in predicting cognitive impairment up to 7.5 years later. Neurology 80, 1784–1791. https://doi.org/10.1212/WNL.0b013e3182918ca6

Scheef, L., Spottke, A., Daerr, M., Joe, A., Striepens, N., Kölsch, H., Popp, J., Daamen, M., Gorris, D., Heneka, M.T., Boecker, H., Biersack, H.J., Maier, W., Schild, H.H., Wagner, M., Jessen, F., 2012. Glucose metabolism, gray matter structure, and memory decline in subjective memory impairment. Neurology 79, 1332–1339. https://doi.org/10.1212/WNL.0b013e31826c1a8d

Sitt, J.D., King, J.-R., El Karoui, I., Rohaut, B., Faugeras, F., Gramfort, A., Cohen, L., Sigman, M., Dehaene, S., Naccache, L., 2014. Large scale screening of neural signatures of consciousness in patients in a vegetative or minimally conscious state. Brain 137, 2258–2270. https://doi.org/10.1093/brain/awu141

Soldan, A., Pettigrew, C., Cai, Q., Wang, M.-C., Moghekar, A.R., O'Brien, R.J., Selnes, O.A., Albert, M.S., for the BIOCARD Research Team, 2016. Hypothetical Preclinical Alzheimer Disease Groups and Longitudinal Cognitive Change. JAMA Neurol. 73, 698. https://doi.org/10.1001/jamaneurol.2016.0194

ten Kate, M., Redolfi, A., Peira, E., Bos, I., Vos, S.J., Vandenberghe, R., Gabel, S., Schaeverbeke, J., Scheltens, P., Blin, O., Richardson, J.C., Bordet, R., Wallin, A.,

Eckerstrom, C., Molinuevo, J.L., Engelborghs, S., Van Broeckhoven, C., Martinez-Lage, P., Popp, J., Tsolaki, M., Verhey, F.R.J., Baird, A.L., Legido-Quigley, C., Bertram, L., Dobricic, V., Zetterberg, H., Lovestone, S., Streffer, J., Bianchetti, S., Novak, G.P., Revillard, J., Gordon, M.F., Xie, Z., Wottschel, V., Frisoni, G., Visser, P.J., Barkhof, F., 2018. MRI predictors of amyloid pathology: results from the EMIF-AD Multimodal Biomarker Discovery study. Alzheimers Res. Ther. 10. https://doi.org/10.1186/s13195-018-0428-1

Vogel, J.W., Vachon-Presseau, E., Pichet Binette, A., Tam, A., Orban, P., La Joie, R., Savard, M., Picard, C., Poirier, J., Bellec, P., Breitner, J.C.S., Villeneuve, S., 2018. Brain properties predict proximity to symptom onset in sporadic Alzheimer's disease. Brain 141, 1871–1883. https://doi.org/10.1093/brain/awy093

Yan, T., Wang, Y., Weng, Z., Du, W., Liu, T., Chen, D., Li, X., Wu, J., Han, Y., 2019. Early-Stage Identification and Pathological Development of Alzheimer's Disease Using Multimodal MRI. J. Alzheimers Dis. 68, 1013–1027. https://doi.org/10.3233/JAD-181049

Yang, S., Bornot, J.M. sanchez, Wong-Lin, K., Prasad, G., 2019. M/EEG-based Bio-markers to predict the Mild Cognitive Impairment and Alzheimer's disease: A Review from the Machine Learning Perspective. IEEE Trans. Biomed. Eng. 1–1. https://doi.org/10.1109/TBME.2019.2898871

Young, A.L., Oxtoby, N.P., Daga, P., Cash, D.M., Fox, N.C., Ourselin, S., Schott, J.M., Alexander, D.C., 2014. A data-driven model of biomarker changes in sporadic Alzheimer's disease. Brain 137, 2564–2577. https://doi.org/10.1093/brain/awu176

Young, J., Modat, M., Cardoso, M.J., Mendelson, A., Cash, D., Ourselin, S., 2013. Accurate multimodal probabilistic prediction of conversion to Alzheimer's disease in patients with mild cognitive impairment. NeuroImage Clin. 2, 735–745. https://doi.org/10.1016/j.nicl.2013.05.004

Yu, H., Lei, X., Song, Z., Wang, J., Wei, X., Yu, B., 2018. Functional brain connectivity in Alzheimer's disease: An EEG study based on permutation disalignment index. Phys. Stat. Mech. Its Appl. 506, 1093–1103. https://doi.org/10.1016/j.physa.2018.05.009

Zhao, W., Luo, Y., Zhao, L., Mok, V., Su, L., Yin, C., Sun, Y., Lu, J., Shi, L., Han, Y., 2019. Automated Brain MRI Volumetry Differentiates Early Stages of Alzheimer's Disease From Normal Aging. J. Geriatr. Psychiatry Neurol. 32, 354–364. https://doi.org/10.1177/0891988719862637

Group number	Name of the group of features	Features inside each group
1	224-channel EEG	PSD delta (224 channels)
		PSD theta (224 channels)
		PSD alpha (224 channels)
		PSD beta (224 channels)
		PSD gamma (224 channels)
		Median spectral frequency (224 channels)
		Spectral entropy (224 channels)
		Algorithmic complexity (224 channels)
		wSMI theta (224 channels)
		wSMI alpha (224 channels)
2	16-channel EEG	PSD delta (16 channels)
		PSD theta (16 channels)
		PSD alpha (16 channels)
		PSD beta (16 channels)
		PSD gamma (16 channels)
		Median spectral frequency (16 channels)
		Spectral entropy (16 channels)
		Algorithmic complexity (16 channels)
3	4-channel EEG	PSD delta (4 channels)
		PSD theta (4 channels)
		PSD alpha (4 channels)
		PSD beta (4 channels)
		PSD gamma (4 channels)
		Median spectral frequency (4 channels)
		Spectral entropy (4 channels)
		Algorithmic complexity (4 channels)
4	Demographic data	Age
		Sex
		Education level
5	APOE4 status	APOE4 status (positive if at least one ε4 allele)
6	Neuropsychological data	MMSE
		FCSRT Immediate Free Recall
		FCSRT Immediate Total Recall
		FCSRT Delayed Free Recall
		FCSRT Delayed Total Recall
		Frontal Assessment Battery
7	Hippocampal Volumetry	Hippocampal Volume on MRI

Table 1: Complete list of features. Abbreviations: FCSRT = Free and Cued Selective Reminding Test; MMSE = Mini Mental Status Examination; PSD = Power spectral density; wSMI = weighted Symbolic Mutual Information.

	All participants	A-	A+	p-value∫
Demographics				
Number of subjects	304	219 (72.04%)	85 (27.96%)	..
Age (years)	76.06 ± 3.48	75.76 ± 3.45	76.81 ± 3.47	0.0180*
Women	191 (62.83%)	137 (62.56%)	54 (63.53%)	0.8749
High educational level§	207 (68.09%)	156 (71.23%)	51 (60.00%)	0.0593
APOE ε4 allele	59 (19.41%)	28 (12.79%)	31 (36.47%)	<0.0001*
Cognitive tests				
Mini-Mental State Examination	28.66 ± 0.96	28.73 ± 0.97	28.47 ± 0.89	0.0329*
Free and Cued Selective Reminding Test				
Immediate Free Recall	29.95 ± 5.45	30.29 ± 5.40	29.06 ± 5.50	0.0764
Immediate Total Recall	46.07 ± 1.98	46.08 ± 2.01	46.05 ± 1.91	0.8897
Delayed Free Recall	11.85 ± 2.28	12.00 ± 2.20	11.47 ± 2.45	0.0718
Delayed Total Recall	15.68 ± 0.63	15.68 ± 0.66	15.68 ± 0.56	0.9803
Frontal Assessment Battery	16.39 ± 1.69	16.53 ± 1.67	16.05 ± 1.68	0.0250*
^{18}F-fluorodeoxyglucose PET				
Mean FDG SUVR†	2.45 ± 0.25	2.47 ± 0.24	2.41 ± 0.25	0.0791
^{18}F-florbetapir PET				
Mean florbetapir SUVR	0.78 ± 0.19	0.69 ± 0.05	1.03 ± 0.20	<0.0001*
Volumetric MRI (cm^3)				
Total hippocampal volume¶	2.71 ± 0.31	2.74 ± 0.30	2.62 ± 0.32	0.0023*

Table 2: Comparison of baseline characteristics between amyloid positive and amyloid negative groups. Data are mean ± SD or number (%). ∫ P-value for the comparison between the two groups. P-values were calculated using Welch's t test for continuous variables and Fisher's exact test for qualitative variables. *P-value < 0.05. †18F-fluorodeoxyglucose PET indices partial-volume corrected. §On a scale of 1–8, where 1=primary education and 8=higher education, high was defined as scores >6. ¶Normalized to the mean total intracranial volume. Abbreviations: A+ = Amyloid positive; A- = Amyloid negative; AD = Alzheimer's disease; FDG = fluorodeoxyglucose; SUVR = standardised uptake value ratio.

Best classifiers to predict amyloid	**RF (10 features) demo+NPSY+APOE+HV**	**RF (all features) demo+NPSY**	**RF (all features) demo+NPSY+APOE+HV**
Rank	1	2	3
Nb (%) selected on 50 iterations	14 (28.00%)	9 (18.00%)	7 (14.00%)
AUC	0.62 [0.50;0.73]	0.51 [0.45;0.73]	0.65 [0.50;0.81]
Balanced accuracy	0.62 [0.50;0.70]	0.53 [0.37;0.69]	0.61 [0.47;0.74]
Sensitivity	0.58 [0.38;0.69]	0.46 [0.26;0.75]	0.46 [0.18;0.81]
Specificity	0.70 [0.46;0.73]	0.58 [0.47;0.67]	0.67 [0.61;0.91]
PPV	0.41 [0.28;0.49]	0.31 [0.17;0.45]	0.40 [0.25;0.50]
NPV	0.80 [0.72;0.86]	0.73 [0.62;0.87]	0.78 [0.70;0.90]
Best classifiers to predict neurodegeneration	**regLOG (5 features) EEG4**	**regLOG (all features) EEG16**	**regLOG (5 features) EEG16**
Rank	1	2	3
Nb (%) selected on 50 iterations	19 (38.00%)	18 (36.00%)	9 (18.00%)
AUC	0.62 [0.53;0.77]	0.68 [0.49;0.84]	0.52 [0.47;0.61]
Balanced accuracy	0.61 [0.45;0.75]	0.60 [0.47;0.76]	0.54 [0.39;0.58]
Sensitivity	0.45 [0.18;0.69]	0.45 [0.17;0.78]	0.36 [0.18;0.53]
Specificity	0.77 [0.59;0.93]	0.73 [0.48;0.87]	0.71 [0.49;0.79]
PPV	0.38 [0.18;0.56]	0.34 [0.17;0.59]	0.29 [0.13;0.33]
NPV	0.82 [0.73;0.89]	0.82 [0.75;0.90]	0.78 [0.70;0.81]

Table 3: Best classifiers to predict amyloid and neurodegeneration status, displayed in ranked order. The following performance measures are indicated: area under operating characteristic (ROC) curve (AUC), balanced accuracy, sensitivity, specificity, positive predictive value (PPV) and negative predictive value (NPV). Performance measures are summarized with median and quantile 0.025 and 0.975. Only the first three best classifiers are indicated. The algorithm, number of features (in brackets) and groups of features used are specified for each classifier. Abbreviations: APOE = APOE4 status; Demo = Demographical data; EEG4 = 4-channel EEG; EEG16 = 16-channel EEG; HV = Hippocampal Volume; Nb = Number; NPSY = Neuropsychological data; RF = Random forest; regLOG = Logistic Regression.

	All participants	N-	N+	p-value∫
Demographics				
Number of subjects	304	232 (76.32%)	72 (23.68%)	..
Age (years)	76.06 ± 3.48	75.92 ± 3.38	76.50 ± 3.78	0.2156
Women	191 (62.83%)	158 (68.10%)	33 (45.83%)	6e-04*
High educational level§	207 (68.09%)	156 (67.24%)	51 (70.83%)	0.5678
APOE ε4 allele	59 (19.41%)	45 (19.40%)	14 (19.44%)	0.9928
Cognitive tests				
Mini-Mental State Examination	28.66 ± 0.96	28.65 ± 0.97	28.69 ± 0.91	0.7108
Free and Cued Selective Reminding Test				
Immediate Free Recall	29.95 ± 5.45	30.16 ± 5.41	29.28 ± 5.56	0.2332
Immediate Total Recall	46.07 ± 1.98	46.17 ± 1.94	45.75 ± 2.07	0.1134
Delayed Free Recall	11.85 ± 2.28	12.00 ± 2.18	11.35 ± 2.55	0.0325*
Delayed Total Recall	15.68 ± 0.63	15.70 ± 0.60	15.62 ± 0.72	0.3891
Frontal Assessment Battery	16.39 ± 1.69	16.38 ± 1.68	16.43 ± 1.71	0.8370
^{18}F-fluorodeoxyglucose PET				
Mean FDG SUVR†	2.45 ± 0.25	2.55 ± 0.20	2.16 ± 0.10	<0.0001*
^{18}F-florbetapir PET				
Mean florbetapir SUVR	0.78 ± 0.19	0.77 ± 0.17	0.84 ± 0.24	0.0060*
Volumetric MRI (cm^3)				
Total hippocampal volume¶	2.71 ± 0.31	2.73 ± 0.32	2.64 ± 0.29	0.0372*

Table 4: Comparison of baseline characteristics between neurodegeneration positive and neurodegeneration negative groups. Data are mean ± SD or number (%). ∫ P-value for the comparison between the two groups. P-values were calculated using Welch's t test for continuous variables and Fisher's exact test for qualitative variables. *P-value < 0.05. †^{18}F-fluorodeoxyglucose PET indices partial-volume corrected. §On a scale of 1–8, where 1=primary education and 8=higher education, high was defined as scores >6. ¶Normalized to the mean total intracranial volume. Abbreviations: AD = Alzheimer's disease; FDG = fluorodeoxyglucose; N+ = neurodegeneration positive; N- = neurodegeneration negative; SUVR = standardised uptake value ratio.

	All participants	AD-decliners	Non-decliners	p-value∫
Demographics				
Number of subjects	248	14 (5.65%)	234 (94.35%)	..
Age (years)	75.73 ± 3.43	77.43 ± 3.67	75.63 ± 3.40	0.0601
Women	148 (59.68%)	7 (50.00%)	141 (60.26%)	0.5765
High educational level§	174 (70.16%)	10 (71.43%)	164 (70.09%)	1.0000
APOE ε4 allele	50 (20.16%)	8 (57.14%)	42 (17.95%)	0.0018*
Cognitive tests				
Mini-Mental State Examination	28.68 ± 0.94	28.21 ± 0.70	28.71 ± 0.95	0.0533
Free and Cued Selective Reminding Test				
Immediate Free Recall	30.12 ± 5.54	24.00 ± 6.29	30.49 ± 5.28	0.0003*
Immediate Total Recall	46.03 ± 2.01	44.64 ± 2.24	46.12 ± 1.97	0.0090*
Delayed Free Recall	15.67 ± 0.65	15.36 ± 0.74	15.69 ± 0.64	0.0238*
Delayed Total Recall	11.83 ± 2.30	9.93 ± 2.89	11.95 ± 2.22	0.0058*
Frontal Assessment Battery	16.47 ± 1.67	16.00 ± 2.11	16.50 ± 1.64	0.4692
Letter verbal fluency in P	22.50 ± 6.07	23.00 ± 6.04	22.47 ± 6.08	0.8885
Category verbal fluency	31.51 ± 7.27	28.71 ± 5.21	31.68 ± 7.35	0.1237
Mean ^{18}F-FDG PET SUVR†	2.46 ± 0.25	2.32 ± 0.23	2.47 ± 0.25	0.0232*
N+ subjects	59 (23.79%)	7 (50.00%)	52 (22.22%)	0.0456*
Mean ^{18}F-florbetapir PET SUVR	0.78 ± 0.19	1.23 ± 0.20	0.75 ± 0.15	<0.0001*
Total hippocampal volume on volumetric MRI (cm^3)¶	2.73 ± 0.30	2.47 ± 0.27	2.74 ± 0.30	0.0005*

Table 5: Comparison of baseline characteristics between participants declining to prodromal AD versus non-decliners during five-year follow-up. Data are mean ± SD or number (%). ∫ P-value for the comparison between the two groups. P-values were calculated using Welch's t test for continuous variables and Fisher's exact test for qualitative variables. *P-value < 0.05. †^{18}F-fluorodeoxyglucose PET indices partial-volume corrected. §On a scale of 1–8, where 1=primary education and 8=higher education, high was defined as scores >6. ¶Normalized to the mean total intracranial volume. Abbreviations: AD = Alzheimer's disease; FCSRT = Free and Cued Selective Reminding Test; FDG = fluorodeoxyglucose; N+ = neurodegeneration positive; SUVR = standardised uptake value ratio.

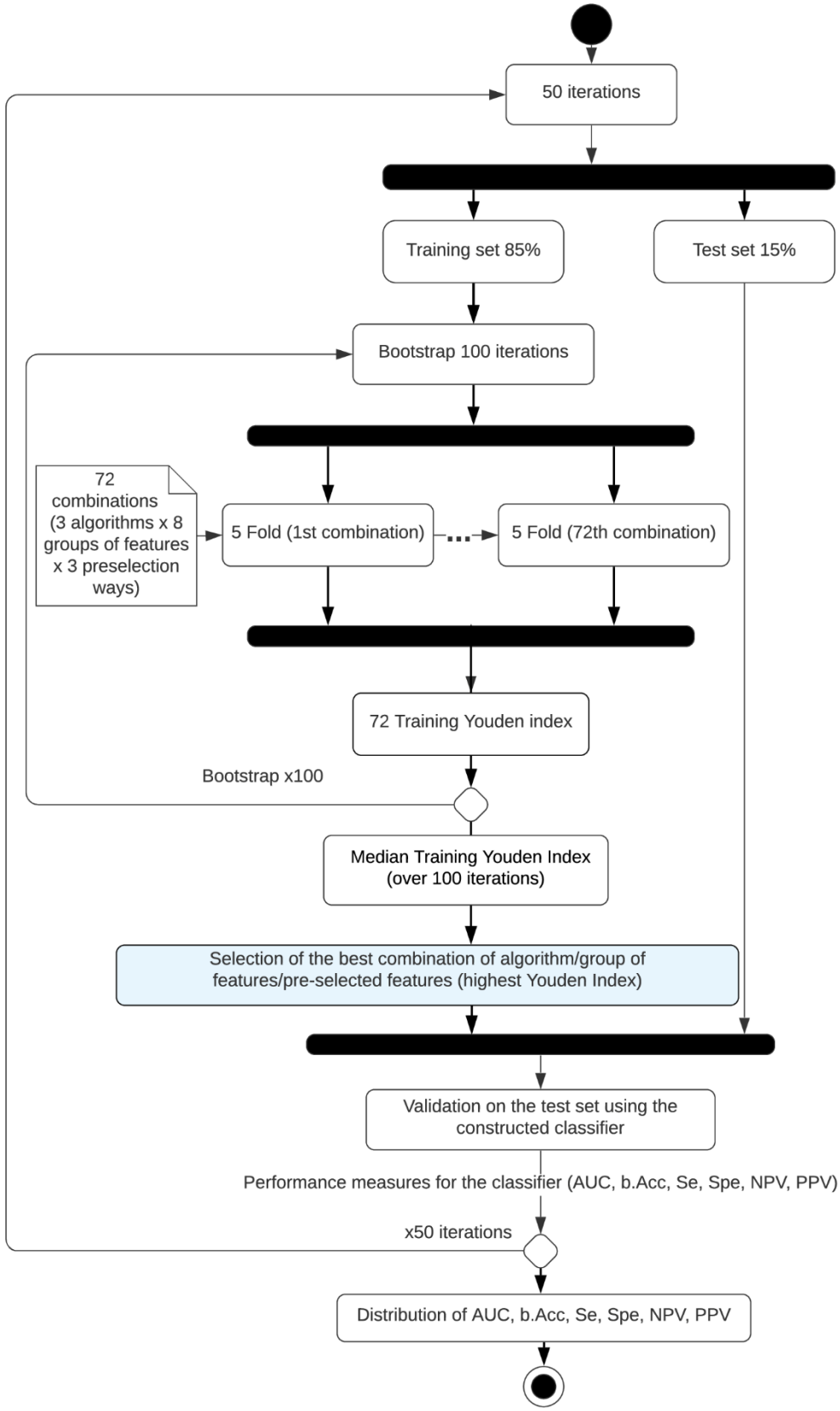

Figure 1: Description of the machine learning pipeline implemented to predict preclinical Alzheimer's disease (AD). Abbreviations: b.Acc = Balanced Accuracy; NPV = Negative Predictive Value; PPV = Positive Predictive Value; Se = Sensitivity; Spe = Specificity.

Supplementary results

3.4.2. Prediction of decline to prodromal AD: an exploratory analysis

3.4.2.1 Best classifier

The best classifier for the prediction of decline to prodromal AD was logistic regression with the following combination of groups of features: demographical, neuropsychological data, APOE4 genotype and hippocampal volumetry (with 5 features pre-selected), enabling a median AUC of 0.70, a 67% balanced accuracy, 50% sensitivity, 83% specificity, 14% PPV and 97% NPV (**Supplementary Table 1**).

3.4.2.2 Best features

The best features for the prediction of decline to prodromal AD were the following (according to the frequency of selection of each feature on 50 iterations): FCSRT Immediate Free Recall (80%), hippocampal volumetry (70%), APOE4 (66%), MMSE (24%), FCSRT Delayed Free Recall (22%), age (20%), education level (20%), sex (20%), FCSRT Delayed Total Recall (20%), FCSRT Immediate Total Recall (20%) and FAB (20%). The other features were selected in a proportion lower than 5%.

Best classifier	regLOG (5 features) demo+NPSY+APOE+ HV	RF (5 features) demo+NPSY+APOE+ HV	RF (all features) Demo+NPSY+APOE+ HV
Rank	1	2	3
Nb (%) selected on 50 iterations	12 (24.00%)	9 (18.00%)	9 (18.00%)
AUC	0.70 [0.58;0.99]	0.67 [0.41;0.97]	0.88 [0.65;0.99]
Balanced accuracy	0.67 [0.45;0.91]	0.65 [0.39;0.94]	0.72 [0.49;0.95]
Sensitivity	0.50 [0.00;1.00]	0.50 [0.00;1.00]	0.50 [0.10;1.00]
Specificity	0.83 [0.58;0.94]	0.86 [0.78;0.91]	0.86 [0.72;0.94]
PPV	0.14 [0.00;0.31]	0.12 [0.00;0.32]	0.20 [0.02;0.39]
NPV	0.97 [0.94;1.00]	0.97 [0.93;1.00]	0.97 [0.95;1.00]

Supplementary Table 1: Best classifiers to predict decline to prodromal AD at 5-year follow-up, displayed in ranked order. The following performance measures are indicated: area under operating characteristic (ROC) curve (AUC), balanced accuracy, sensitivity, specificity, positive predictive value (PPV) and negative predictive value (NPV). Performance measures are summarized with median and quantile 0.025 and 0.975. Only the first three best classifiers are indicated. The algorithm, number of features (in brackets) and groups of features used are specified for each classifier.

Abbreviations: APOE = APOE4 status; Demo = Demographical data; EEG4 = 4-channel EEG; EEG16 = 16-channel EEG; HV = Hippocampal Volume; Nb = Number; NPSY = Neuropsychological data; RF = Random forest; regLOG = Logistic Regression.

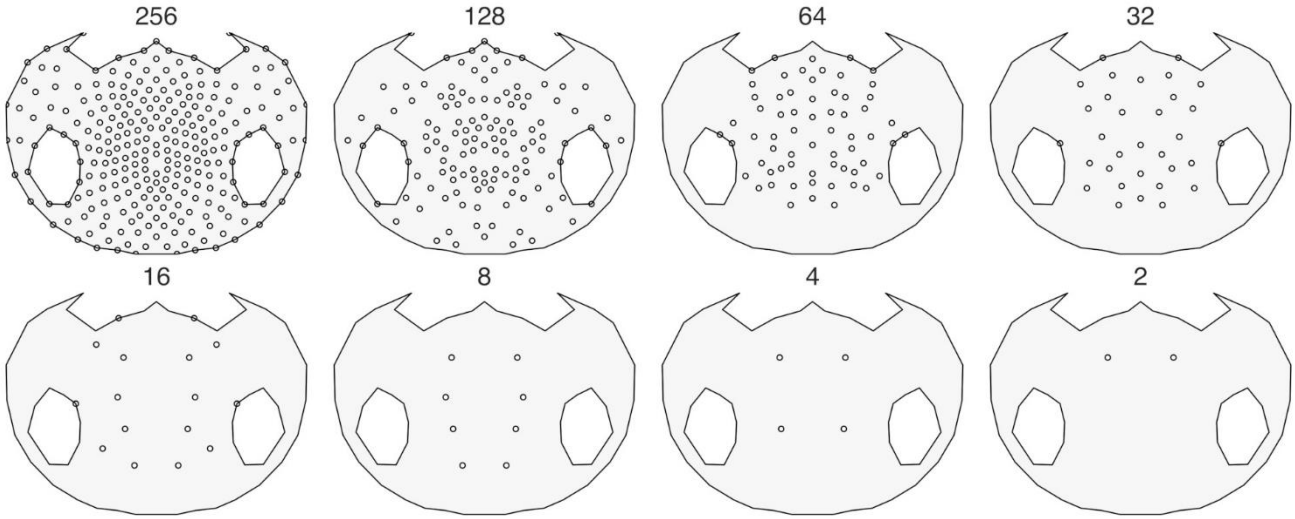

Supplementary Figure 1: Different EEG configurations with progressive reduction of the number of channels (256, 128, 64, 32, 16, 8, 4, 2)

HIGHLIGHTS

- Quantitative EEG best predicts neurodegeneration in preclinical Alzheimer's disease
- Portable low-density EEG is a promising tool to predict neurodegeneration
- Demographic, cognitive data, APOE4 and hippocampal volumetry best predict amyloid
- Verbal memory, hippocampal volume and APOE4 predict cognitive decline at 5 years
- Machine learning can help to screen for preclinical Alzheimer's disease